Simplified Modeling of Brazing Furnaces

Academic Coordinator Elena Martín Ortega
University University of Vigo and Technological Institute for Industrial Mathematics (ITMATI)

Business Coordinators Anxo Feijóo Lorenzo and Jose Carlos Pérez Ramillo
Companys Ecomanagement Technology and BorgWarner

Specialist Fernando Varas Mérida
University Technical University of Madrid (UPM)

Team Ashwin Sadanand Nayak (University of A Coruña and ITMATI), Hayley Wragg (University of Bath), Youssef Fathallah (University of Santiago de Compostela), Mª Dolores Gómez Pedreira, José Luis Ferrín González (University of Santiago de Compostela and ITMATI), Nerea Vilela Barreira and Damián Bazarra Castro (EcoMT) and Carlos Coroas Fombella (University of Vigo)

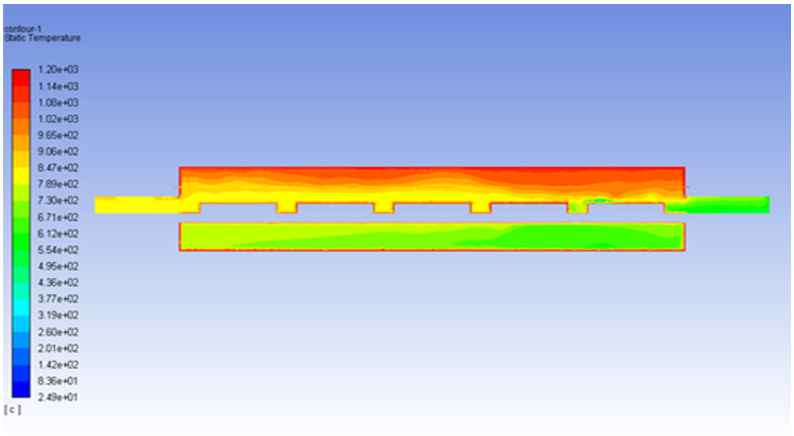

Simplified Modeling of Brazing Furnaces

E. Martín[1], A. S. Nayak[2] and F. Varas[3]

Abstract

This work tackles different modeling approaches to describe the brazing process of automotive stainless steel pieces inside continuous furnaces with controlled (reducing) atmosphere. In particular, three different models, which are complementary between them, are described. The first one, a global zone model, describes the mass flow exchanges and simplified energy balances between the different zones present in this type of furnaces. The second one is a (more) detailed zone model, where each zone is decomposed in various sub-zones (control volumes) for which different energy balances (for the gases, pieces and furnace walls) and mass conservation equations of gaseous species (H_2 and H_2O) are imposed. Finally, the third method presented consists on a CFD numerical model of the muffle region of the furnace. After the necessary validation process, these approaches can lead to a good understanding of the thermal conditions and local atmosphere present inside the different regions of the furnace and can potentially be used to predict the effects caused by any change in an operational parameter (e.g. the mass flow injection of H_2, injection location, conveyor velocity, ...) of the furnace. However, prediction of the quality of the brazing process along specific regions of the pieces would require much more detailed models that are out of the scope of this work.

[1] University of Vigo and ITMATI; emortega@uvigo.es
[2] University of Coruña; ashwin.nayak@udc.es
[3] Technical University of Madrid (UPM); fernando.varas@upm.es

1. Introduction to the brazing process

The use of controlled atmosphere continuous furnaces for brazing of stainless steel pieces is increasing with rising demand of stainless steel parts by manufacturers of aerospace and automotive industries.

The brazing process (see [1] for a complete reference) is a joining manufacturing process between metal parts that uses a filling metal (paste, ring or foils of copper alloy, nickel-chromium-boron alloys etc.). The filling is deposited on the metal junction and the set is then submitted to a high temperature in a furnace in order to melt the filling material. By capillary effect on the walls of the narrow gap between the parts to be joined, the filling enters the junction and a metal alloy is formed in the process of solidification and, consequently, the metals pieces are joined, as described in figure 1. The filler metal must have a lower melting temperature than the materials it is joining and must be of a similar base to them.

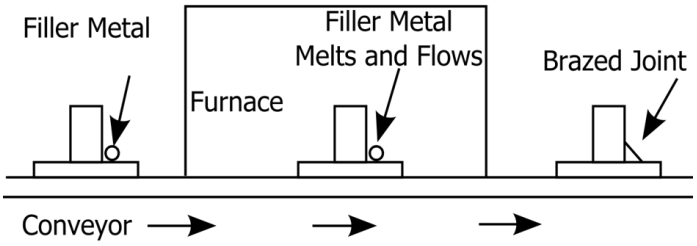

Figure 1: Simplified diagram of the brazing process.

The key to a successful brazing is the preparation of the surface. Contaminant elements and metal oxides prevent the filler metal from forming an alloy with the metals of the parts to be processed. Also, in case of little oxidation, the pores of the surface to be processed will be closed by the oxide, preventing the capillary action and the brazing itself. This is why the furnace atmosphere needs to be reducing in the brazing process and maintained so in a controlled fashion. Keeping the surface of the parts in the furnace reduced is much more difficult for brazing of stainless steel parts than for brazing of mild steel parts. In particular, the chromium in the stainless steel creates a much more stable oxide at an oxygen level much lower than that of carbon steel.

The oxide on the surface must be reduced before reaching the melting temperature of the filler. Usually this reduction is made through a reaction of hydrogen with the oxygen present in the metal oxide, forming water vapor (1).

$$M_xO_y + yH_2 \underset{b}{\overset{f}{\rightleftarrows}} xM + yH_2O \tag{1}$$

Too much water vapor (or oxygen) in the system prevent the reaction from continuing and, therefore, from reducing the oxide. To determine the water

vapor levels inside the furnace atmosphere the dew point is used. The dew point is the temperature at which a quantity of water vapor in the system saturates the atmosphere and condenses, forming little water drops. Usually the dew point required for brazing of stainless steel junctions in a high concentration hydrogen atmosphere is very low, which requires very high furnace temperatures at the brazing zone [1]. As an example, for AISI 300 series stainless steel, the required dew point is $-50°C$ and the brazing temperature is usually between 1040 and 1100°C in atmosphere with high concentration of hydrogen ($\sim$ 75-80%) if the brazing is performed with copper or nickel-chromium–phosphorus, and pure hydrogen (100%) if nickel-chromium-boron filler or silicon are used.

The continuous furnace with controlled atmosphere is the economically best way for brazing of high quantity of pieces in stainless steel. An sketch of a typical brazing furnace and its main regions is shown in figure 2 along with their corresponding temperature-time diagram.

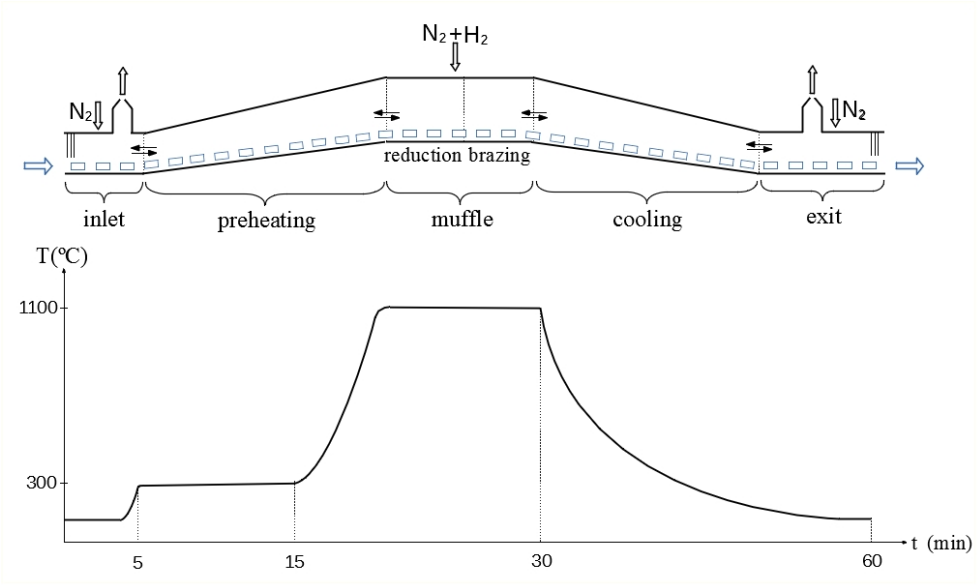

Figure 2: Sketch of a continuous brazing furnace and its common parts: pieces inlet (with curtain), inlet hood, preheating zone, muffle, cooling zone, outlet hood, and pieces outlet (with curtain).

The temperature–time relation is the first step to achieve a good product quality. The thermal energy provided by the furnace is used for different functions. The part to be processed has to be heated first at a temperature at which the surface oxide of the base metal can be reduced as a result of the reaction of the present iron oxides and the reducing components of the controlled atmosphere. Extra energy is necessary to melt the filler metal and form an alloy with the base metal. As for copper and AISI 300 series stainless

steel, the variation of the temperature for the brazing is between $1090-1100°C$ and for nickel-chromium alloys it is between $1080-1130°C$. This temperature depends on the shape and composition of the brazing metal, on the type of component and its assembly, as well as on other operating conditions, such as speed of the conveyor belt or the length of the heating zone.

The local reducing atmosphere present at the muffle zone is fundamental to achieve a correct brazing. Therefore, the optimal configuration implies working with a furnace in positive operation pressure to avoid air infiltration inside the furnace. Taking into account the high cost of H_2, controlling the efficiency of the furnace is vital. Thus, information concerning the flow along the doors as well as internal flows between different parts of the furnaces and its dependency with other operational conditions (atmospheric humidity and pressure inside the plant, H_2 mass flow injection, ...) is crucial.

2. Simplified Modeling

ECOMT[1](A Coruña, Spain) is a leading company in monitoring data for different productive industrial processes to control and improve the energy efficiency of different installations. As a demand to improve the efficiency of the brazing process for their client BorgWarner Emissions Systems Spain S.L.[2] (Vigo, Spain), a leading industry provider of automotive parts, the team centered its objective in designing the steps needed for developing a "digital twin" of the furnace which responds like a real furnace installed in the client company (see figure 3)

Figure 3: Example of arrangement of the pieces on the conveyor at the furnace inlet (left) and picture of a complete furnace line (right) installed at Borgwarner Emissions Systems Spain S.L. Company.

The final model aims to give an insight on the real distribution of the

[1] https://ecomt.net
[2] https://www.borgwarner.com/company/locations/vigo

reducing atmosphere inside the furnace and its dependence on the injected hydrogen mass flow.

2.1. Global Zone Model

The global zone model tries to capture the mean values of the flow properties for each one of the six zones of the furnaces (as indicated in figure 2): inlet, preheating, reduction and brazing sections of the muffle, cooling and exit zones. For each zone, balances of mass flow for each species and energy should be solved. Therefore, the variables considered for the global zone model would be

- Averaged temperature for each zone
- Averaged concentration of H_2 and H_2O for each zone
- Averaged working piece temperature at each piece position
- Concentration of trapped H_2O inside each piece at each piece position

The last variable is relevant for the brazing process as it is has been observed that the dew point inside the muffle is sensible to the local atmospheric conditions in the plant. Thus, the kinetics of the reduction/oxidation reaction is affected by this parameter and, consequently, the final quality of the brazing.

A direct approach to obtain the total mass flow exchanged between zones would be to solve a simple hydraulic network that allows to relate mass flows to differences of pressure between the regions. Once the total mass flows are obtained, the next step would be to solve the energy balance and the distribution of the mass flow between the three different gases H_2, H_2O and N_2 for each zone. Some of the parameters included in this model (e.g. the parameters needed to configure the head losses in the hydraulic network) would need calibration through sensors and experimental measurements extracted from the industrial furnace.

Results of this model can be satisfactory when applied to certain control tasks. However, the global model cannot retain all the details needed to ensure a correct brazing process. As the model only deals with averaged temperature and concentrations of H_2 and H_2O inside each zone, the information provided by the model is clearly insufficient to relate to the quality of the brazing.

Therefore, more complicated models are presented below. The first one, a detailed (and more accurate) zone model, is presented in the next section 2.2. The second one, a computational fluid dynamics (CFD) model of the muffle region, which uses (partially) some information extracted from the global zone mode, will be described in section 2.3. Likewise, some information post-processed from the CFD model can be used as inputs in the detailed zone model, as we will see later.

2.2. Detailed Zone Model

This model considers each of the six different zones (or at least the muffle region) divided into N number of different control volumes (depending on the level of details aimed to be retained) as in figure 4. For each control volume, energy balances are solved, having the same variables as in the global zone model but extended along each control volume. To determine the exchange of H_2 and H_2O mass flows between adjacent control volumes ($\dot{m}_{i,i'}$ in the equations that follow), conservation balances of mass and momentum should be imposed. Unfortunately, this approach is not precise enough to characterize the flows, due to the complex mechanisms involved in the thermal-fluid dynamic problem. Instead, a more accurate approach would be to approximate these fluxes with the results from the CFD model, post-processed for each control volume. Also, additional parameters involved in the detailed zone model should be modeled numerically or, alternatively, estimated experimentally.

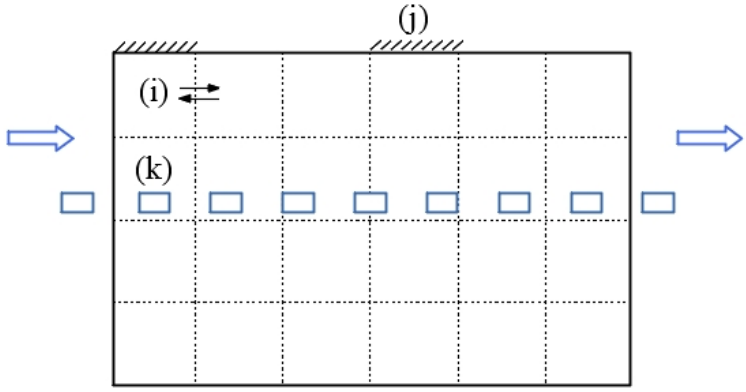

Figure 4: Sketch of the different control volumes in the muffle region.

Thus, a model with N control volumes ($i = 1, 2, ..., N$), a total number S_w of solid surfaces over the furnace walls ($j = 1, 2, ..., S_w$) and a total of K different pieces positions ($k = 1, 2, ..., K$) is then considered. Each energy and mass flow balance will be explained as follows.

2.2.1 Energy balance at each control volume

Following the work of Tan et al. [2], the energy balance for the i–th control volume (see figure 5) can be expressed by the following equation (2), assuming

a steady temperature for the gases and the furnace walls:

$$\sum_{\substack{i'=1,\\ i\neq i'}}^{N} \overleftrightarrow{G_i G_{i'}}\ \sigma T^4_{vc(i')} + \sum_{j=1}^{S_w} G_i S_j \sigma T^4_{wall(j)} + \sum_{k=1}^{K} G_i \hat{S}_k \sigma T^4_{wp(k)} - aV_i \sigma T^4_{vc(i)} -$$

$$- \sum_{\substack{interfaces,\\ (i)-(i'')}} c_p{}^g \dot{m}_{i,i"} T_{ve(\substack{upwind\\ i,i"})} - \sum_{\substack{working\ pieces\ in\\ control\ volume(k)}} c_p^{wp}\ \frac{m_{wp}}{t_{res}} (T_{wp(k)} - T_{wp(k-1)}) = 0 \quad (2)$$

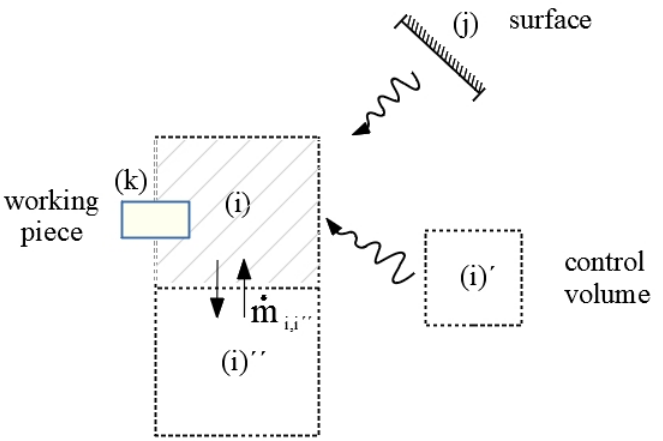

Figure 5: Sketch of the different interactions that take place in the energy balance inside a control volume.

The first three terms account for the thermal radiation that the gas receives from the gas inside the other zones, from the furnace walls and from the pieces, respectively. The fourth term takes into account the thermal radiation emitted from the gas in the i–th control volume. The fifth term accounts for the convective heat transport between control volumes, while the last term represents the enthalpy variation of the pieces that cross the control volume.

2.2.2 Energy balance on each work piece

This balance represents the enthalpy variation of the pieces as they move across the furnace. The pieces heating or cooling will be the result of the right hand term of equation (3), which takes into account, respectively, the radiation coming from the furnace walls, radiation coming from the gas of different control volumes and from other positions, the heat exchanged with the gases and the thermal radiation emitted by the piece in this position k (see figure

6):

$$c_p{}^{wp}\ \frac{m_{wp}}{t_{res}}(T_{wp(k)} - T_{wp(k-1)}) = \sum_{j'=1}^{S_w} \overleftarrow{\hat{S}_k S_{j'}}\ \sigma T^4_{wall(j')} + \sum_{i'=1}^{N} \overleftarrow{\hat{S}_k G_{i'}}\ \sigma T^4_{cv(i')} +$$
$$+ \sum_{\substack{k'=1,\\ k'\neq k}}^{K} \overleftarrow{\hat{S}_k \hat{S}_{k'}}\ \sigma T^4_{wp(k')} + \hat{A}_k h_k (T_{vc(i)} - T_{wp(k)}) - \hat{A}_k \epsilon_k \sigma T^4_{wp(i)} \quad (3)$$

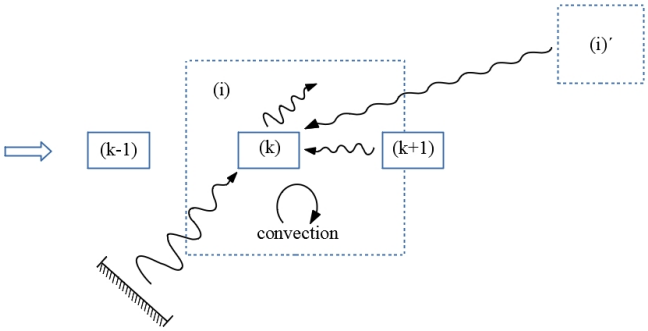

Figure 6: Interactions in the energy balance for each piece

2.2.3 Energy balance on wall surfaces

The following equation (4) shows the thermal balance for a given part (j–th surface) of the internal furnace walls (as depicted in figure 7). This equation describes the contributions, in a steady operational regime, to the energy equation, where Q_j, which is the heat generated by the electrical resistances, balances the radiation fluxes (coming from other furnace walls, pieces and gases as well as the outgoing flux from the wall) and the convective fluxes (from the gases inside the furnace and exchange through the exterior walls of the furnace)

$$Q_j = \sum_{\substack{j'=1\\ j'\neq j}}^{S_w} \overleftarrow{S_j S_{j'}}\ \sigma T^4_{wall(j')} + \sum_{k=1}^{K} \overleftarrow{S_j \hat{S}_k}\ \sigma T^4_{wp(k)} + \sum_{i=1}^{N} \overleftarrow{S_j G_i}\ \sigma T^4_{cv(i)} -$$
$$-A_j \epsilon_j \sigma T^4_{wall(j)} + \sum_{\substack{control\ volumes\\ in\ contact}} A_{j,i}\ h_j (T_{cv}(i) - T_j) - -A_j h_j{}^{ext}(T_j - T_{room}) \quad (4)$$

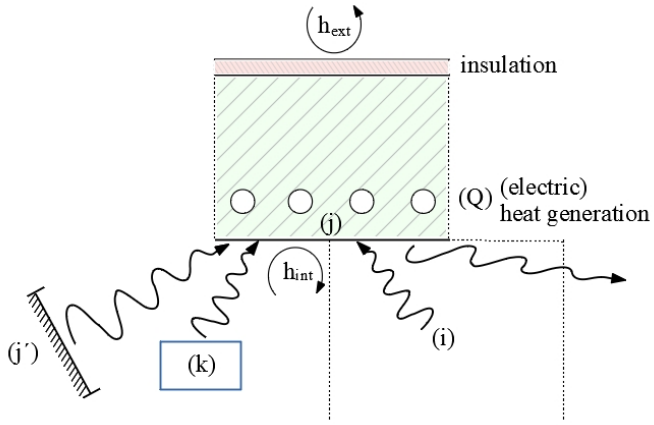

Figure 7: Interaction on a section of the furnace walls

2.2.4 H_2 mass flow balance in a control volume

Over each gas control volume (see figure 8), the mass flow balance of H_2 could be given by equation (5). The injection of H_2 in this control volume, W_i, should be equal to the H_2 mass flow exchanged with the neighboring control volumes and the rates of generation and consumption of H_2 in the reduction/oxidation equation (1).

$$W_i = \sum_{\substack{neighbouring \\ control\ volumes}} \dot{m}_{i,i'}[H_2]_{i'} + \sum_{\substack{working \\ pieces\ in \\ control\ volume}} A_{wp(k)}[k_f(T_{wp(k)}([H_2]_i{}^a - k_b(T_{wp(k)})[H_20]_i{}^b] \quad (5)$$

For the last terms, the kinetics of the forward (reduction) reaction, k_f, and backward (oxidation) reaction, k_b, has been taken into account:

$$r_f = k_f(T)[H_2]^a \quad (6)$$

$$r_b = k_b(T)[H_2O]^b \quad (7)$$

2.2.5 H_2O balance in a control volume

The water vapor mass flow balance in a control volume (as in figure 9) comes from the exchange with neighboring regions, the net rate of generation/consumption from the reduction/oxidation equation and the water vapor freed from the void

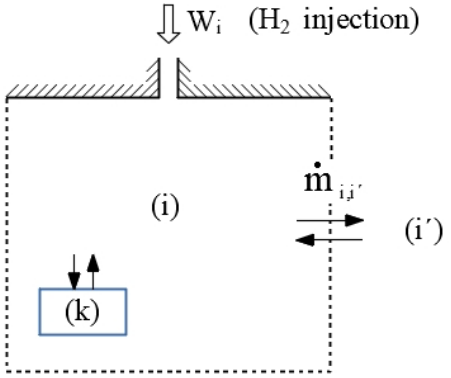

Figure 8: Sketch of a control volume with injection of H_2

inside the pieces, as indicated by equation (8).

$$
\begin{aligned}
0 = & \sum_{\substack{neighbouring \\ control\ volumes}} \dot{m}_{i,i'}[H_2O]_{i'} \\
& + \sum_{\substack{working \\ pieces\ in \\ control\ volume}} A_{wp(k)}[k_d T_{wp(k)}[H_2]_i{}^a - k_i T_{wp(k)}[H_2O]_i{}^b] + \\
& + \sum_{\substack{working \\ pieces\ in \\ control\ volume}} [\dot{H_2O}]_{wp(k)}
\end{aligned} \tag{8}
$$

As in the previous section, the kinetics associated to the release of trapped H_2O must be also taken into account:

$$
[\dot{H_2O}]_{wp(k)} = -k_{wr}(T_{wp(k)})[H_2O]^c{}_{wp(k)} \tag{9}
$$

2.3. CFD model of the muffle

As in the zonal models described in the previous sections, similar hypotheses were used to formulate a simplified model for the muffle thermal simulation (see [3] for a similar modeling in a different type of industrial furnace). Except for the obvious transient character of the pieces thermal problem, it is assumed that the furnace operates under steady conditions. Thus, temperature fields for furnace walls in the furnace chamber are both assumed to be steady. At the same time, the gases inside the muffle were considered to be not participating in the thermal radiation. Therefore, thermal radiation is then

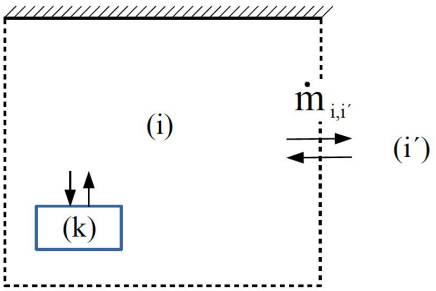

Figure 9: Example of a H_2O mass flow balance for a control volume.

reduced to a surface–to–surface problem restricted to solid surfaces (furnace walls, workpieces surfaces and conveyor belt surface).

The complete model will be decomposed in three submodels concerning, respectively: (a) heat transfer in furnace walls and radiating surfaces, (b) thermo-fluid dynamics of H_2, H_2O and N_2 gases inside the muffle chamber, and (c) heating of the pieces itself. In this section, each of these submodels (as well as its coupling in order to obtain the global CFD model) will be presented.

2.3.1 Thermal model for the furnace walls

According to the previously stated hypotheses, a steady conduction problem must be solved on the furnace walls domain. The furnace walls are formed by some materials with specific (non uniform) thermal conductivity k_s. As this material is object to degradation of its thermal properties between maintenance periods, it seems relevant to include it in the thermal evaluation of the problem. Electric resistances, uniformly distributed inside the furnace, generate a net constant heat source Q when working under steady operational conditions. On the external boundary, cooling by the ambient will be described using a very simple model where heat transfer coefficient h is to be adjusted in order to describe local cooling conditions (and T_∞ stands for the local ambient temperature in the industrial plant). Also, a layer of insulation material is expected to be present near the external surface. In turn, heat exchange through internal walls will be obtained by the composition of a convective heat flux (from the gases inside the furnace) q_{conv} and a (net) radiation heat flux q_{rad}.

$$-\nabla \cdot (k_s \nabla T_s) = Q \tag{10}$$

$$-k_s \frac{\partial T_s}{\partial n} = h(T_s - T_\infty) \qquad \text{on} \quad \Gamma_{ext} \tag{11}$$

$$-k_s \frac{\partial T_s}{\partial n} = q_{conv} + q_{rad} \qquad \text{on} \quad \Gamma_{int} \tag{12}$$

In order to obtain the radiation heat flux on a surface element (assuming that the total radiative surface has been decomposed into N_{rad} elements) we have for the net radiation heat flux (on the k–th surface element)

$$q^k_{rad} = \sigma \epsilon_k \left(T^4_k - \frac{1}{\epsilon_k A_k} \sum_{j=1}^{N_{rad}} G_{jk} A_j \epsilon_j T^4_j \right) \tag{13}$$

as a function of Gebhart factors, G_{jk}, temperatures, T_j, emissivities, ϵ_j, and areas, A_j, of all the radiative surfaces in the enclosure.

The set of radiative surfaces is composed by all the interior walls of the furnace, including the conveyor belt and the workpieces surfaces. In order to compute the radiation heat flux, the workpieces surface temperature will be obtained from the corresponding submodel (see below).

2.3.2 Thermal model for the furnace gases

A second submodel corresponding to the gases domain inside the furnace must be solved to describe heat transfer from gases in the muffled chamber in order to obtain the Reynolds-averaged density, ρ_g, velocity, $\vec{U}$, and temperature, T_g, of the gases. The thermo–hydrodynamical (steady) model for the mixture of gases is described by Reynolds–averaged compressible Navier–Stokes equations and the energy conservation equation (for non–reactive gases), for which the turbulent Reynolds stress tensor τ^R is described by a standard $k-\epsilon$ model as follows

$$\nabla \cdot \left(\rho_g \vec{U} \right) = 0 \tag{14}$$

$$\nabla \cdot \left(\rho_g \vec{U} \otimes \vec{U} \right) + \nabla P - \nabla \cdot \left(\mu_g (\nabla \vec{U} + (\nabla \vec{U})^T \right) = \nabla \cdot \tau^R \tag{15}$$

$$\tau^R = \rho_g \nu_T \left(\nabla \vec{U} + (\nabla \vec{U})^T \right) \quad \text{with} \quad \nu_T = C_\mu \frac{k^2}{\epsilon} \tag{16}$$

$$\nabla \cdot \left(\rho_g c_g \vec{U} T_g \right) - \nabla \cdot \left((k_g + \rho_g c_g \frac{\nu_T}{Pr_t}) \nabla T_g \right) = 0 \tag{17}$$

$$\nabla \cdot \left(\rho_g \vec{U} k \right) - \nabla \cdot \left((\mu_g + \rho_g \frac{\nu_T}{\sigma_k}) \nabla k \right) = \tau^R : \nabla \vec{U} - \rho_g \epsilon \tag{18}$$

$$\nabla \cdot \left(\rho_g \vec{U} \epsilon \right) - \nabla \cdot \left((\mu_g + \frac{\rho_g \nu_T}{\sigma_\epsilon}) \nabla \epsilon \right) = C_{\epsilon 1} \frac{\epsilon}{k} \tau^R : \nabla \vec{U} - C_{\epsilon 2} \rho_g \frac{\epsilon^2}{k} \rho_g \epsilon \tag{19}$$

where Pr_t was chosen equal to 0.9 while the rest of the constants involved in the turbulent model (C_μ, σ_k, σ_ϵ, $C_{\epsilon 1}$ and $C_{\epsilon 2}$) were equal to the standard ones. μ_g, k_g and c_g stand for gases viscosity, thermal conductivity and specific heat, respectively.

The gases mixture will be formed by $N(=3)$ species: N_2, H_2 and H_2O. The latter two are driven by the reduction (forward) or oxidation (backward) reaction (1) that takes place at the piece surface. For inox steels, the metal more prone to form oxides is Cr.

The ideal gas relationship for the mixture (of molecular weight W)

$$P = \frac{\rho_g}{W} R_u T_g \tag{20}$$

should be completed with the mass fraction equations Y_i for each species i, such that:

$$\rho_g = \sum_i^N \rho_i Y_i \tag{21}$$

$$W = \frac{1}{\sum_i^N \frac{Y_i}{W_i}} \tag{22}$$

where only $N-1$ mass fraction transport equations need to be computed (due to $\sum_i^N Y_i = 1$ mass conservation property):

$$\nabla \cdot \left(\rho_g \vec{U} Y_i \right) - \nabla \cdot \left(\rho_g (D_i + \frac{\nu_T}{Sc_t}) \nabla Y_i \right) = 0 \tag{23}$$

being the turbulent Schmidt number Sc_t commonly taken equal to Pr_t.

Equations (17) and (23) represent the energy and mass transport equation for nonreactive species in the gases domain (right-hand terms in the equations equal to 0). However, the numerical model might take into account the production and consumption terms for H_2 and H_2O with the appropriate boundary conditions at the surfaces of the pieces. As an example, the cells in contact with the pieces have a source term for the transport equation of H_2 equal to:

$$S_{H_2} = -\rho_g W_{H_2} \left(k_f(T_g) \left[\frac{\rho_g Y_{H_2}}{W_{H_2}} \right]^y - k_b(T_g) \left[\frac{\rho_g Y_{H_2O}}{W_{H_2O}} \right]^y \right) \tag{24}$$

where k_f and k_b stand for the constants of the forward and backward reaction given by eq. (1).

Standard wall laws can be applied for furnace internal walls and workpieces surfaces boundary conditions where the wall temperature is obtained from the solution of the corresponding submodels. At the mass flow injection inlets, temperature, composition and velocity of the gases mixture are to be imposed. Inlet turbulent parameters should also be specified.

Boundary conditions of temperature, composition, velocity of the gases mixture and/or pressure at the pieces inlet and outlet zones are critical as they account for the global gas flow inside the complete furnace. A good idea seems to combine the information given by the global zone model with the CFD model through the boundary conditions in these sections.

2.3.3 Thermal model for the workpieces

Finally, a model describing heating of steel workpieces in the furnace must be provided. This model will be given by the transient heat equation (25) for the piece temperature field T_p and the suitable boundary conditions for the heat transfer at the pieces walls (26)

$$\rho_p c_p(T_p)\frac{\partial T_p}{\partial t} - \nabla \cdot (k_p(T_p)\nabla T_p) = 0 \tag{25}$$

$$-k_p(T_p)\frac{\partial T_p}{\partial n} = q_{rad} + q_{conv} \tag{26}$$

where q_{rad} and q_{conv} stand for radiation and convective, respectively, heat flow. In order to avoid the difficulties of a moving mesh problem, the pieces are considered to occupy fixed positions inside the computational domain during a given residence time, that is, the total residence time of each piece inside the muffle divided by the number of pieces inside the muffle region. For a given piece position (k), the initial temperature field of the piece will be given by the final temperature field acquired from position ($k-1$) and so on.

In this model, q_{rad} and q_{conv} will be obtained from the previous submodels. A conduction term q_{cond} (corresponding to conduction from the conveyor belt) must be added if the contact surface between pieces and conveyor belt is significant.

2.3.4 Simplified CFD thermal model for the muffle

As an example of the possibilities of the CFD model, a simplified problem was tackled during the modeling week by the team. In particular, submodel in section 2.3.2 for the gases for a unique-component gas was solved for the computational domain of figure 10 with the academic version of software Ansys/Fluent©. Uniform temperatures for the furnace walls and for the conveyor belt respectively were prescribed following the data provided by EcoMT. A prescribed temperature curve for the pieces was also imposed. Specific mass flow rates at the gases injection area were taken from real data of the furnace operation. Concerning the pieces inlet and outlet, different values of the pressure were prescribed to mimic either incoming or outgoing flows through these boundaries. These boundary conditions represent the coupling between the global zonal mode and the muffle CFD model for the proposed

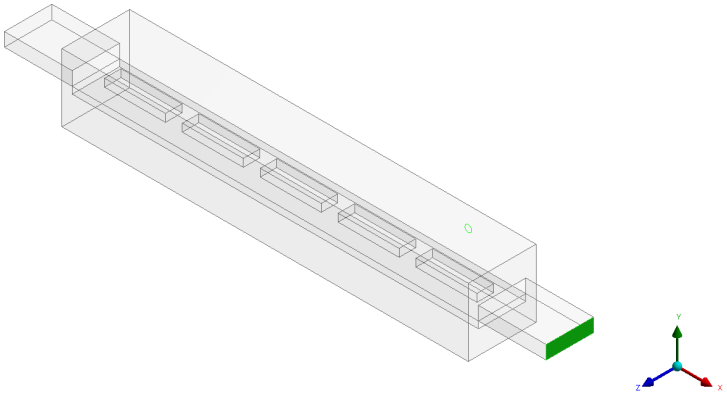

Figure 10: Example of simplified computational domain for the muffle zone.

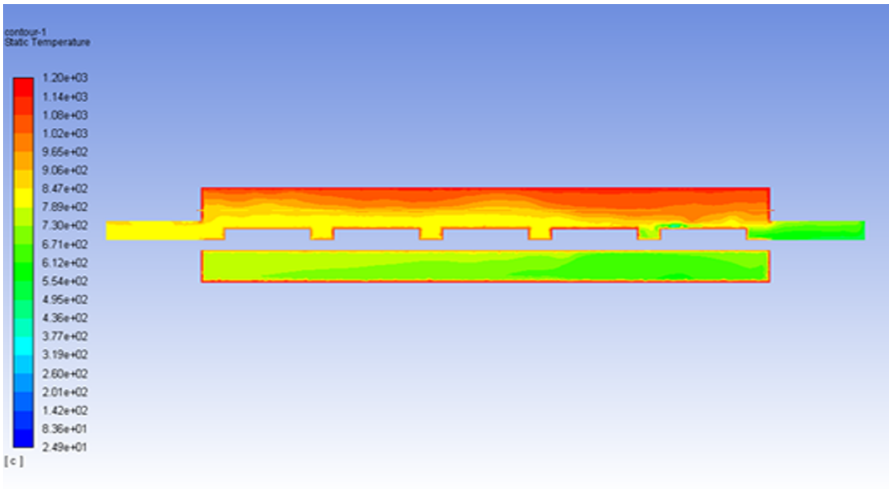

Figure 11: Computational temperature field in the middle plane of the muffle.

approach. Some of the results for the temperature and velocity fields are shown in figures 11 and 12, respectively. The last figure shows the complex velocity patterns that can be found inside the muffle region even for a very simplified model. It is to be remarked (see figure 12 right) that the injected flow is able to provide both a cooling effect of the brazed parts near the injection and a reducing atmosphere in the first part of the muffle.

The results of the complete CFD model, will provide the suitable mass flow distributions to feed, with reliable data, each of the different control volumes considered in the detailed zonal approach.

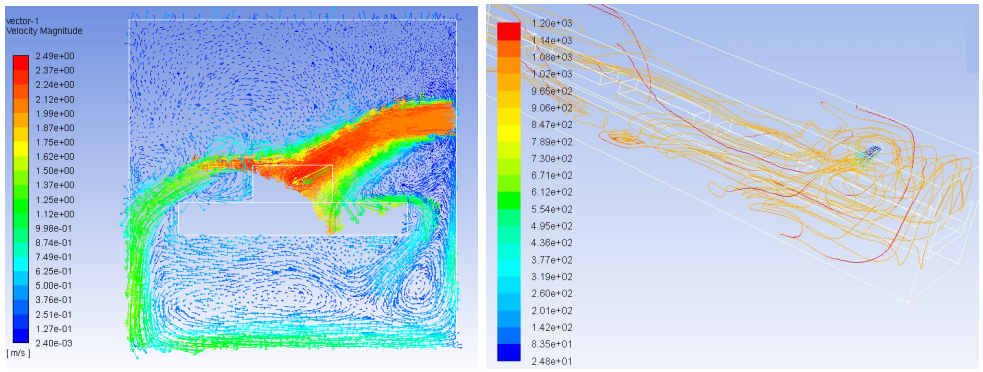

Figure 12: Computational velocity vector field over the piece for a transversal plane located at the H_2 injection area (left). Path lines coming from the H_2 injection (right), colored by temperature.

3. Conclusions

Different models have been presented to mimic the behavior of the complex thermal-fluid dynamic processes involved inside a brazing furnace: a global zone modeling that account for all the six different zones of the process (inlet, pre-heating, reducing, brazing, cooling and exit), a more detailed zone modeling with a decomposition of (at least) the muffle region in different sub-zones (control volumes), and a complex CFD simulation of the muffle region.

These models are complementary, that is, some outputs of the global model are needed as boundary conditions for the CFD of the muffle and, at the same time, some (post-processed) outputs of the CFD model can be used as inputs for the detailed zonal mode.

Some of the parameters involved in the modeling need to be calibrated from measurements from the plant (e.g. parameters of the hydraulic network of the global zone model). Likewise, the whole modeling should be validated through experimental tests (using, for example, DataPaq® measurements for working piece temperatures).

After the necessary validation process, these approaches can lead to a well understanding of the local concentrations of the different gaseous species involved in the problem under different conditions. They can also help to predict the effects generated by the change of a specific operational parameter (e.g. the mass flow injection of H_2, its injection location, conveyor velocity, ...)

However, the models presented are quite far from predicting the brazing process performance in detail, as the problem involves surface tension-driven flows (with dynamic contact lines with variable surface tension due to reactive melting) as well as strong effects of the local thermal pattern on the reactive (due to the allow formation) wetting process, which require much more detailed

models.

References

[1] P. M. Roberts, Introduction to Brazing Technology *Taylor & Fracis Group*, CRC Press 2016.

[2] C. Tan, J. Jenkins, J. Ward, J. Broughton, A. Heeley, Zone modelling of the thermal performances of a large-scale bloom reheating furnace, *Applied Thermal Engineering*, vol. 50, pp. 1111-1118, 2013.

[3] E. Martín, M. Meis, C. Mourenza, D. Rivas, F. Varas, Fast solution of direct and inverse design problems concerning furnace operation conditions in steel industry, *Applied Thermal Engineering*, vol. 47, pp. 41-53, 2012.